Cost of Diffusion: Nonlinearity and Giant Fluctuations

Satya N. Majumdar,[1] Francesco Mori,[2] and Pierpaolo Vivo[3]

[1]*LPTMS, CNRS, Université Paris-Sud, Université Paris-Saclay, 91405 Orsay, France*

[2]*Rudolf Peierls Centre for Theoretical Physics, University of Oxford, Oxford OX1 3RH, United Kingdom*

[3]*Department of Mathematics, King's College London, London WC2R 2LS, United Kingdom*

(Received 10 February 2023; revised 14 April 2023; accepted 15 May 2023; published 8 June 2023)

We introduce a simple model of diffusive jump process where a fee is charged for each jump. The nonlinear cost function is such that slow jumps incur a flat fee, while for fast jumps the cost is proportional to the velocity of the jump. The model—inspired by the way taxi meters work—exhibits a very rich behavior. The cost for trajectories of equal length and equal duration exhibits giant fluctuations at a critical value of the scaled distance traveled. Furthermore, the full distribution of the cost until the target is reached exhibits an interesting "freezing" transition in the large-deviation regime. All the analytical results are corroborated by numerical simulations. Our results also apply to elastic systems near the depinning transition, when driven by a random force.

DOI: 10.1103/PhysRevLett.130.237102

Introduction.—For more than a century, simple stochastic processes like the random walk have been successfully used to model a variety of phenomena across disciplines [1–3]. For instance, the motion of bacteria in space [1,2] and the evolution of the price of a stock in finance [3] can be approximated as a sequence of jumps between *states*, which take place according to some probabilistic rule.

In many different contexts, it is natural to associate a (possibly nonlinear) cost—or a reward—to the "change of state" of a stochastic process—often with unexpected or paradoxical consequences. For instance, the energy consumption of bacteria changes depending on the environment they move in [1]. Wireless devices absorb different amounts of energy when they switch between activity states (off, idle, transmit, or receive) [4,5]. In biochemical reactions, it is often convenient to label secondary reaction products as cost or reward of an underlying primary process [6] for bookkeeping purposes. The *bonus-malus* vehicle insurance premium changes depending on the number of claims made in the previous year [7]. In software development, the so-called "technical debt" is the cost of additional rework caused by prioritizing an easy solution now instead of a better design approach that would delay the release of the product [8]. In a variety of situations where random factors are present that affect the change of state of a system, computing the total cost (or reward) of a trajectory may prove very challenging.

In mathematics and engineering, stochastic processes with associated costs have been investigated in the framework of Markov reward models [9–11]. Recently, the joint distribution of displacement and cost has also been investigated in Ref. [12] for random walks in a random environment until a first-passage event. Moreover, optimal control theory has been applied in Ref. [13] to minimize the cost of random walks with resetting. However, the impact of a nonlinear cost function on the cost fluctuations, both in the typical and in the large deviation regime, remains largely unexplored.

An everyday example where nonlinear costs lead to unexpected consequences is that of taxi fares. Indeed, taxi rides in a busy city typically consist of a mixture of fast excursions and slow steps due, e.g., to congestion or traffic lights. The fare charged to a passenger is automatically computed by the taxi meter, which follows a fairly universal and simple recipe [14]. Each city council determines a *changeover speed* η_c—based on a statistical analysis of the typical local traffic conditions. If the taxi moves faster than η_c, the meter ticks according to the *space* covered, while if the taxi moves slower than η_c, the meter ticks according to the *time* elapsed. This way, the driver gets compensated even when the taxi barely moves due to heavy traffic. For example, according to London's Tariff I rate [15] the meter should charge 20 pence for every 105.4 m covered, or 22.7 sec elapsed (whichever is reached first). One of the surprising consequences of the nonlinear nature of the taxi fare structure is the so-called *taxi paradox* [14], whereby two taxis starting together from A and arriving together at B may charge very different fares depending on their individual patterns of slow versus fast chunks in their trajectories.

In this Letter, we study a simple but general model of diffusion, inspired by the taxi paradox, where the nonlinear nature of the costs associated to each jump gives rise to a rich and nontrivial behavior. In particular, we will consider two scenarios: fixing both the total distance X and the number n of steps [ensemble (i)] or fixing the target location L but allowing the number of steps to get there to fluctuate [ensemble (ii)]. In ensemble (i), the cost has a finite and nonmonotonic variance, which is maximal at some critical value of the scaled distance X/n. In ensemble (ii), we show that the cost variance displays a rich behavior when changing the speed threshold η_c, including "giant" fluctuations of the total cost. In this latter setting, the large deviations of the hitting cost displays an unexpected "freezing" transition in the low-cost regime. Our results show that associating a nonlinear cost to the evolution of a random walk leads to very rich and unexpected phenomena.

Model.—Consider a one-dimensional walker whose position X_n at discrete time n evolves according to

$$X_n = X_{n-1} + \eta_n \tag{1}$$

starting from the origin $X_0 = 0$, with η_n drawn independently from a probability density function $p(\eta)$ with positive support. To each jump, we associate a cost C_n that increases according to the law

$$C_n = C_{n-1} + h(\eta_n), \tag{2}$$

where $h(\eta)$ is a function of η. The final position reached after n steps is $X = \sum_{k=1}^{n} \eta_k$, and the total cost due is $C = \sum_{k=1}^{n} h(\eta_k)$. For a typical realization of the process, see Fig. 1. Clearly, X and C are correlated random variables, whose joint statistics is of interest here.

We further assume that the jumps are positive and exponentially distributed with mean value μ, i.e., that $p(\eta) = \exp(-\eta/\mu)/\mu$. For simplicity, we set $\mu = 1$.

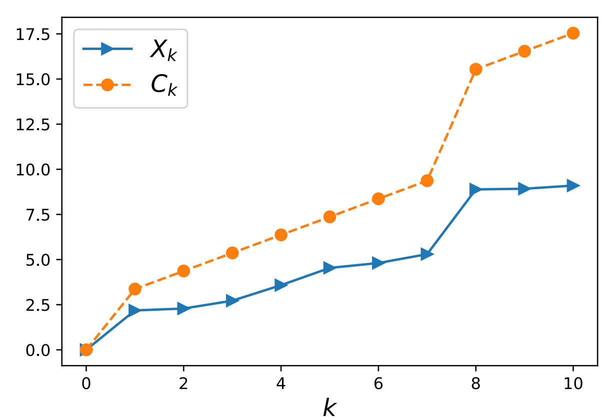

FIG. 1. Typical realization of a random walk X_k with cost function $h(\eta) = 1 + 2(\eta - 1)\theta(\eta - 1)$. The cost C_k up to step k is a nonlinear function of the random jumps.

Inspired by the taxi paradox described above, we consider the nonlinear cost function $h(\eta) = 1 + b(\eta - \eta_c)\theta(\eta - \eta_c)$, with $b > 0$ a positive constant, and $\theta(x)$ the Heaviside step function. This function $h(\eta)$ is such that jumps shorter than the critical size η_c in one unit of time (*slower* jumps) incur a unit fee, whereas longer (*faster*) jumps are more costly, with the fee being proportional to the length (velocity) of the jump. Thus, in our model there are two parameters, b and η_c.

Main results [ensemble (i)].—Because of the nonlinear nature of the cost function, even after fixing the total distance X and the number of steps n, the total cost C remains random, as expressed by the taxi paradox. For large n, the average cost grows with the total distance X as

$$\langle C \rangle_{X,n} \approx n + b\eta_c n H\left(\frac{X}{n\eta_c}\right), \tag{3}$$

where $H(y) = ye^{-1/y}$. To quantify the cost fluctuations around the average, we first compute the cost variance $\mathrm{Var}(C|X,n)$ conditioned on the value of X after exactly n steps. In particular, in the late-time limit $n \to \infty$, $X \to \infty$ with $y = X/(n\eta_c)$ fixed, we find that the variance takes the scaling form,

$$\mathrm{Var}(C|X,n) \approx b^2\eta_c^2 n F\left(\frac{X}{n\eta_c}\right), \tag{4}$$

where

$$F(y) = e^{-2/y}(2e^{1/y}y^2 - 2y^2 - 2y - 1) \tag{5}$$

is a positive, nonmonotonic scaling function. This scaling function is shown in Fig. 2 and it is in perfect agreement

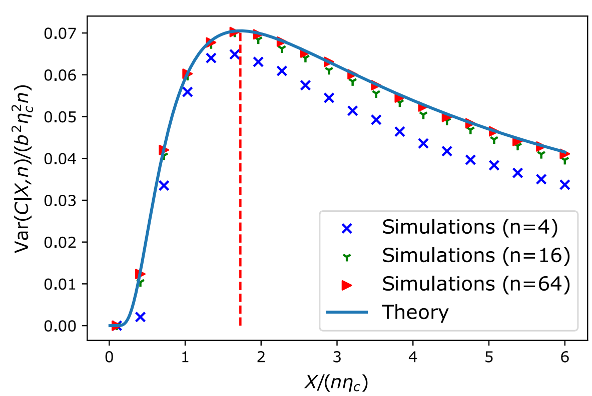

FIG. 2. Scaled cost variance $\mathrm{Var}(C|X,n)/(b^2\eta_c^2 n)$ conditioned on the final position X as a function of $X/(n\eta_c)$. The continuous blue line corresponds to the analytical scaling function in Eq. (5) (valid for $n \to \infty$). The symbols display the results of numerical simulations with 10^5 samples and different values of n. The vertical dashed line highlights the maximum at $X/(n\eta_c) \approx 1.727\,24...$.

with numerical simulations. Note that the variance has a single maximum at the point $y^\star \approx 1.727\,24\ldots$. This scaling function has asymptotic behaviors $F(y) \approx 2y^2 e^{-1/y}$ for small y and $F(y) \approx (1/3y)$ for large y.

To understand the nonmonotonic behavior of the variance, consider two opposite limits: $X \gg n\eta_c$ (that is y large) and $X \ll n\eta_c$ (y small). In the former case, when X is fixed to be large, in a typical trajectory, most of the jumps are big; i.e., the configuration is dominated by "spacelike" runs only (i.e., $\eta_i > \eta_c$) and hence the cost can be written as $C = \sum_i [1 + b(\eta_i - \eta_c)] \approx n + b(X - n\eta_c)$. Consequently, since both n and X are fixed, the fluctuations of C are severely constrained for large X. This decrease in the cost fluctuations is hence a consequence of the linearity of $h(\eta)$ for large η (see Supplemental Material [16] for a discussion on the nonlinear case). In the latter case $X \ll n\eta_c$, a typical trajectory is dominated by only "timelike" runs and once again the cost fluctuations from one trajectory to another are expected to be small, as the precise length of each jump will not significantly alter the fee charged per jump. Thus these two "phases" are like "pure" phases. As one increases the control parameter $X/(n\eta_c)$, one first crosses over from a timelike pure phase to a "mixed" phase, characterized by a larger entropy (i.e., a larger number of possible arrangements of individual jumps eventually landing to the same final spot X after n jumps). Upon further increasing $X/(n\eta_c)$, the conditional variance undergoes a second crossover from the mixed phase to a spacelike pure phase. At the special value $X/(n\eta_c) \approx 1.727\,24\ldots$, the cost fluctuations are maximal (the most unfair scenario for taxi passengers).

Physical applications.—Nonlinear functions similar to $h(\eta)$, composed of a constant and a linear part, naturally emerge in disparate areas of physics. An elementary example is that of static friction: in order to move a block in contact with a substrate one has to overcome a threshold force η_c due to static adhesion. Then, applying a force η for a fixed time interval Δt, the velocity of the block is given by $h(\eta) = b(\eta - \eta_c)\theta(\eta - \eta_c)$, where b now depends on the block mass and Δt [17]. The function $h(\eta)$ is the velocity-force characteristic describing the response of the system to an applied force and, up to a global shift by 1, is identical to the cost function per unit time in our taxi model. A natural question is, what is the average response when the block is subject to a *random applied force* η drawn from, say, $p(\eta) = e^{-\eta}$? To measure this average (over random force) response, one needs to repeat the experiment n times, by applying a random force η_i drawn independently for each sample i from $p(\eta)$. Then $X_n/n = (1/n)\sum_{i=1}^n \eta_i$ is precisely the mean force per sample, and $C_n/n = (1/n)\sum_{i=1}^n h(\eta_i)$ is the mean velocity of the block per sample. Thus, the number of steps n in the taxi problem plays the role of the number of samples here. Consequently, for large n, the scaling function $H(y) = ye^{-1/y}$ in Eq. (3) describes precisely the average response characteristic, while $F(y)$ in Eqs. (4) and (5) describe the fluctuations of the response around its average.

More generally, our results can be extended to a wide variety of disordered systems when an extended object or manifold such as an elastic string or a polymer is driven by a random force η in a spatially inhomogeneous medium. These systems undergo a depinning transition when a force η is applied: below the depinning threshold η_c, the manifold is pinned by the disorder and its velocity vanishes, while above the threshold, the velocity-force relation follows a power-law scaling $h(\eta) \propto (\eta - \eta_c)^\beta$ with the depinning exponent $\beta > 0$ [18–20]. For example, when a DNA chain translocates through a nanopore by applying a pulling force via optical tweezer, the exponent $\beta \approx 1$ [21], while for a harmonic elastic string in $(1+1)$ dimensions one gets $\beta \approx 0.33$ [19]. Other examples include vortices in type-II superconductors [22] and colloidal crystals [23]. To analyze the velocity-force characteristic for such an elastic string driven by a random force, we need to generalize our method presented above for $\beta = 1$ to $h(\eta) = b(\eta - \eta_c)^\beta$ for arbitrary $\beta > 0$. In Supplemental Material [16], we have computed exactly both the average velocity-force response characteristic and its fluctuations for arbitrary β. Our results show that the associated scaling functions $H_\beta(y)$ and $F_\beta(y)$ depend continuously on β.

Main results [ensemble (ii)].—It is also natural to estimate the distribution $P(C|L)$ of the *hitting cost* to be paid to reach a given location L, irrespective of the time required. First-passage or hitting properties [24–26] are important in several applications, from chemical reactions [27] to insurance policies [28]. Note that in this second setting, the number n of steps is a random variable. We find that for large L the distribution of C takes the large-deviation form,

$$P(C|L) \sim \exp[-L\Phi(C/L)], \tag{6}$$

where the rate function reads

$$\Phi(z) = \max_s[-sz + 1 + u(s)] \tag{7}$$

and $u(s)$ satisfies

$$bs + (bse^s - 1)u - u^2 e^s - bse^{u\eta_c} = 0. \tag{8}$$

The rate function $\Phi(z)$ is supported over $z \in [\ell_1(b), \infty)$ and has the following asymptotic behaviors [16]:

$$\Phi(z) \approx \begin{cases} z\ln z - z + 1 & z \to \infty \\ \frac{(z-a_1)^2}{2\sigma_C^2} & z \sim a_1 \\ \psi_b(z) & z \to \ell_1(b), \end{cases} \tag{9}$$

where $\ell_1(b)$ and $\psi_b(z)$ are given below [see Eq. (11)]. Thus, in the typical regime, the cost fluctuates around the typical value $C = a_1 L$, where $a_1 = 1 + b\exp(-\eta_c)$, with variance $\mathrm{Var}(C|L) = L\sigma_C^2$, where

$$\sigma_C^2 = 1 + 2b^2 e^{-\eta_c}(1 - e^{-\eta_c}) - 2b\eta_c e^{-\eta_c}(1 + be^{-\eta_c}). \quad (10)$$

It turns out that the cost variance σ_C^2 has a surprisingly rich behavior as a function of the parameters η_c and b. First, for both $\eta_c \to 0$ and $\eta_c \to \infty$ the scaled variance σ_C^2 tends to the limiting value 1 (see Fig. 3). This counterintuitive result can be understood as follows. For $\eta_c \to \infty$, all of the steps are timelike and hence the cost $C = n$, where n is the number of steps. The distribution $P(n|L)$ of the number of steps n needed—given the target location L—is Poisson, $P(n|L) = e^{-L}L^{n-1}/(n-1)!$ for $n = 1, 2, \ldots$ (see Supplemental Material [16] for the derivation). Therefore, $\mathrm{Var}(C|L) = \mathrm{Var}(n|L) = L$. On the other hand, for $\eta_c \to 0$, all of the steps are spacelike and hence $C = n + bL$, where L is the final position. Thus, we obtain again $\mathrm{Var}(C|L) \approx \mathrm{Var}(n|L) = L$.

For intermediate values of η_c, the behavior of σ_C^2 depends on b. For small values of b, σ_C^2 has a unique minimum as a function of η (see Supplemental Material [16]). Interestingly, above the critical value $b > b_c \approx 2.953\ldots$ (that we computed numerically with *Mathematica*), σ_C^2 develops a second minimum and a maximum (see Fig. 3). This behavior can be qualitatively understood as follows: for η_c slightly above zero, most of the steps are still spacelike. Therefore, $C = \sum_{k=1}^{n} h(\eta_k) \approx bL + (1 - b\eta_c)n$, hence the variance $\mathrm{Var}(C|L) \approx (1 - b\eta_c)^2 L$, implying that $\sigma_C^2 = (1 - b\eta_c)^2$ initially must decrease linearly as η_c increases from zero. As η_c increases further, timelike steps become more and more abundant. The cost fluctuations start increasing again with increasing η_c and become maximal at some $\eta_c^\star$. These giant fluctuations reflect the perfect mixing of timelike and spacelike steps, which can be arranged in the maximal number of different ways to cover the distance L. Increasing η_c further beyond the maximum leads the cost fluctuations to subside, as the pure timelike phase settles in.

The behavior of the lowest edge $\ell_1(b)$ of the support of $\Phi(z)$ is also very interesting. First, the edge $\ell_1(b)$ itself depends on whether b is smaller or larger than $1/\eta_c$. More precisely, $\ell_1(b) = b$ for $b \le 1/\eta_c$, while $\ell_1(b) = 1/\eta_c$ for $b \ge 1/\eta_c$. Around the lower edge, we have the following behavior for $z \to \ell_1(b)^+$:

$$\psi_b(z) = \begin{cases} 1 + \frac{z-b}{1-b\eta_c}\ln\left(\frac{z-b}{1-b\eta_c}\right) - \frac{z-b}{1-b\eta_c} & b < 1/\eta_c \\ -2\sqrt{\delta_1}\sqrt{z-b} + 1 + \delta_0 & b = 1/\eta_c \\ -\frac{1}{\eta_c}\ln\left(z - \frac{1}{\eta_c}\right) + \mathcal{O}(1) & b > 1/\eta_c, \end{cases} \quad (11)$$

with δ_0 solution of $\delta_0 + e^{\delta_0/b} = 0$ and $\delta_1 = \delta_0^2/(b - \delta_0)$. Therefore, the rate function $\Phi(z)$ attains a finite value at the lower edge of its support, $\ell_1(b) = b$, if $b \le 1/\eta_c$, whereas it diverges logarithmically at the lower edge of its support, $\ell_1(b) = 1/\eta_c$, if $b > 1/\eta_c$. A plot of the full rate function computed by solving Eqs. (7) and (8) numerically with *Mathematica*, along with the asymptotic behaviors above, is included in Fig. 4 for different values of b and $\eta_c = 1$.

Interestingly, the lower edge $\ell_1(b)$ "freezes" to the value $\ell_1(b) = 1/\eta_c$ for $b > 1/\eta_c$. To understand this freezing transition, we notice that the lower edge $\ell_1(b)$ is related to the minimal possible cost $C_{\min}$ by $\ell_1(b) = C_{\min}/L$. In Supplemental Material [16], we show that if $b < 1/\eta_c$, i.e., when spacelike configurations are sufficiently inexpensive, the cost is minimized by a single long jump of length $\eta = L$, corresponding to $C_{\min} \approx bL$ [and hence $\ell_1(b) = b$]. On the other hand, for $b > 1/\eta_c$, the minimal cost $C_{\min} = n = L/\eta_c$ is attained with $n = L/\eta_c$ timelike steps of length η_c leading to $\ell_1(b) = 1/\eta_c$.

Derivations.—We focus on the probability $P(C, X|n)$ that a random walker has reached position X after exactly n steps with a total cost C [ensemble (i)]. This quantity can be formally written as

$$P(C, X|n) = \left\langle \delta\left(X - \sum_{k=1}^{n}\eta_k\right)\delta\left(C - \sum_{k=1}^{n} h(\eta_k)\right)\right\rangle, \quad (12)$$

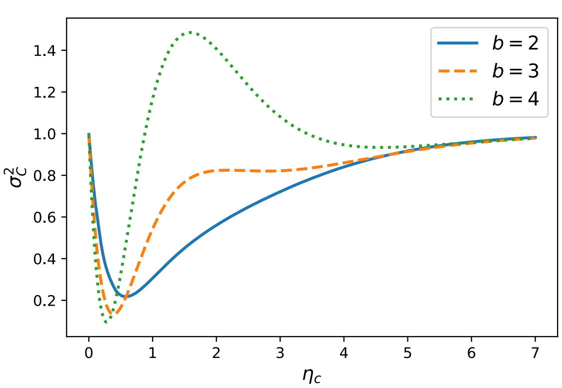

FIG. 3. Variance σ_C^2 of the hitting cost as a function of η_c for increasing values of b.

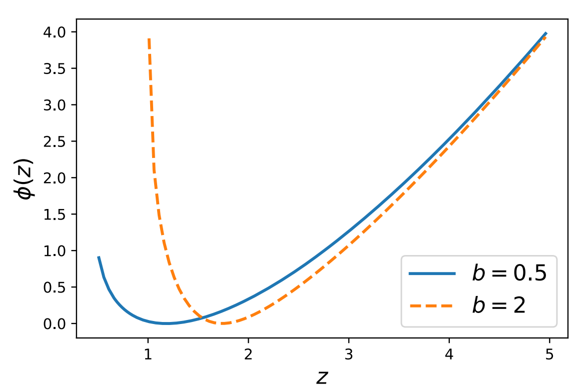

FIG. 4. Rate function $\Phi(z)$ describing the large deviations of the hitting cost, evaluated by solving Eqs. (7) and (8) numerically with *Mathematica* for $\eta_c = 1$ and $b = 0.5$ (continuous line) and $\eta_c = 1$ and $b = 2$ (dashed line).

where the average is performed over the variables η_i. Taking the double Laplace transform $\tilde{P}(\lambda, s|n) = \int_0^\infty P(C, X|n) \times e^{-\lambda X - sC} dX dC$ yields [16] $\tilde{P}(\lambda, s|n) = [g(\lambda, s)]^n$, where

$$g(\lambda, s) = \frac{e^{-s}}{\lambda+1}\left[1 - \frac{bs}{\lambda+1+bs} e^{-(\lambda+1)\eta_c}\right]. \quad (13)$$

The distribution of the final position alone is easily obtained as $P(X|n) = [1/\Gamma(n)] X^{n-1} e^{-X}$ for an exponential jump distribution. Thus, the kth moment of C, conditioned on the total displacement X, can be obtained by Laplace inversion [16], leading to the exact expressions for the average and variance of the cost in Eqs. (39) and (42) of Supplemental Material [16]. The fact that the conditional variance is nonzero embodies the taxi paradox described earlier, as different trajectories reaching the same spot after the same number of steps (= time) may indeed charge different amounts.

Conclusions and outlook.—Motivated by the taxi paradox, we have introduced and solved exactly a simple model for diffusion with a nonlinear cost associated to each jump. Our results exhibit unexpected phenomena, including giant fluctuations of the cost and a freezing transition in the large deviation regime of the total cost. We expect that our results should apply generally to arbitrary jump distributions $p(\eta)$ with a finite variance. We have shown that our results can be directly applied to a variety of physical systems where an extended object is pulled by a random force in a disordered medium. In future works, it would be interesting to investigate fat-tailed jump distributions such as Lévy walks, which are of central importance in finance and biology [29]. In particular, very fat-tailed jump distribution will display condensation phenomena, where a single jump dominates the trajectory [30]. It would be relevant to investigate the impact of a nonlinear cost on such setting. Moreover, one may consider cost functions that penalize short jumps and rewards instead long excursions with a flat fee—a pattern commonly found in public transportation pricing models, where monthly passes are typically cheaper than collecting single ride tickets.

This work was supported by a Leverhulme Trust International Professorship Grant (No. LIP-2020-014).

[1] H. C. Berg, *Random Walks in Biology* (Princeton University Press, Princeton, NJ, 2018).

[2] E. A. Codling, M. J. Plank, and S. Benhamou, Random walk models in biology, J. R. Soc. Interface **5**, 813 (2008).

[3] J.-P. Bouchaud, The subtle nature of financial random walks, Chaos **15**, 026104 (2005).

[4] P. J. M. Havinga and G. J. M. Smit, Energy-efficient wireless networking for multimedia applications, Wireless Commun. Mobile Comput. **1**, 165 (2001).

[5] L. Cloth, J.-P. Katoen, M. Khattri, and R. Pulungan, Model checking Markov reward models with impulse rewards, in *Proceedings of the 2005 International Conference on Dependable Systems and Networks (DSN'05), Yokohama, Japan* (IEEE, Yokohama, 2005), pp. 722–731, 10.1109/DSN.2005.64.

[6] A. Angius and A. Horváth, Analysis of stochastic reaction networks with Markov reward models, in *Proceedings of the 9th International Conference on Computational Methods in Systems Biology (CMSB '11)* (Association for Computing Machinery, New York, 2011), pp. 45–54, 10.1145/2037509.2037517.

[7] G. Amico, J. Janssen, and R. Manca, Discrete time Markov reward processes a motor car insurance example, Technol. Invest. **1**, 135 (2010).

[8] V. Lenarduzzi, T. Besker, D. Taibi, A. Martini, and F. Arcelli Fontana, A systematic literature review on Technical Debt prioritization: Strategies, processes, factors, and tools, J. Syst. Software **171**, 110827 (2021).

[9] R. Howard, *Dynamic Probabilistic Systems* (Wiley, New York, 1971), Vol. 1–2.

[10] L. Tan, K. Mahdaviani, and A. Khisti, Markov rewards processes with impulse rewards and absorbing states, arXiv:2105.00330.

[11] A. Gouberman and M. Siegle, Markov reward models and Markov decision processes in discrete and continuous time: Performance evaluation and optimization, in *Lecture Notes in Computer Science*, Vol. 8453, edited by A. Remke and M. Stoelinga (Springer, Berlin, 2014), 10.1007/978-3-662-45489-3_6.

[12] A. Bianchi, G. Cristadoro, and G. Pozzoli, Ladder costs for random walks in Lévy media, arXiv:2206.02271.

[13] B. De Bruyne and F. Mori, Resetting in stochastic optimal control, Phys. Rev. Res. **5**, 013122 (2023).

[14] R. Eastaway and J. Wyndham, *How Long is a Piece of String?: More Hidden Mathematics of Everyday Life* (Pavilion Books, London, 2005).

[15] https://tfl.gov.uk/modes/taxis-and-minicabs/taxi-fares/tariffs.

[16] See Supplemental Material at http://link.aps.org/supplemental/10.1103/PhysRevLett.130.237102 for further details on the analytical computations.

[17] A. Vanossi, N. Manini, and E. Tosatti, Static and dynamic friction in sliding colloidal monolayers, Proc. Natl. Acad. Sci. U.S.A. **109**, 16429 (2012).

[18] C. Pascal, T. Giamarchi, and P. Le Doussal, Creep and depinning in disordered media, Phys. Rev. B **62**, 6241 (2000).

[19] O. Duemmer and W. Krauth, Critical exponents of the driven elastic string in a disordered medium, Phys. Rev. E **71**, 061601 (2005).

[20] C. Reichhardt and C. J. O. Reichhardt, Depinning and nonequilibrium dynamic phases of particle assemblies driven over random and ordered substrates: A review, Rep. Prog. Phys. **80**, 026501 (2016).

[21] T. Menais, Polymer translocation under a pulling force: Scaling arguments and threshold forces, Phys. Rev. E **97**, 022501 (2018).

[22] G. Blatter, M. V. Feigel'man, V. B. Geshkenbein, A. I. Larkin, and V. M. Vinokur, Vortices in high-temperature superconductors, Rev. Mod. Phys. **66**, 1125 (1994).

[23] A. Pertsinidis and X. S. Ling, Statics and Dynamics of 2D Colloidal Crystals in a Random Pinning Potential, Phys. Rev. Lett. **100**, 028303 (2008).

[24] S. Redner, *A Guide to First-Passage Processes* (Cambridge University Press, Cambridge, England, 2001).
[25] A. J. Bray, S. N. Majumdar, and G. Schehr, Persistence and first-passage properties in non-equilibrium systems, Adv. Phys. **62**, 225 (2013).
[26] S. N. Majumdar, Brownian functionals in physics and computer science, Curr. Sci. **89**, 2076 (2005).
[27] P. Hänggi, P. Talkner, and M. Borkovec, Reaction-rate theory: Fifty years after Kramers, Rev. Mod. Phys. **62**, 251 (1990).
[28] F. Avram, Z. Palmowski, and M. R. Pistorius, Exit problem of a two-dimensional risk process from the quadrant: Exact and asymptotic results, Ann. Appl. Probab. **18**, 2421 (2008).
[29] V. Zaburdaev, S. Denisov, and J. Klafter, Lévy walks, Rev. Mod. Phys. **87**, 483 (2015).
[30] S. N. Majumdar, M. R. Evans, and R. K. P. Zia, Nature of the Condensate in Mass Transport Models, Phys. Rev. Lett. **94**, 180601 (2005).